An Optimal PV System Fed Water Pump Three Phase Induction Motor without Storage Systems Based on TLBO Technique and ANN

MAHMOUD M. ELKHOLY , AHMED FATHY
Electrical Power and Machines Department
Faculty of Engineering, Zagazig University
EGYPT
melkholy71@yahoo.com, afali@zu.edu.eg

Abstract: - In this paper an optimal performance of three phase induction motor drives a centrifugal water pump and fed from PV system without storage elements during starting and running is presented. A three level three phase inverter is used to convert the dc voltage from the PV array to a variable voltage and frequency to supply the three phase induction motor. The output voltage and frequency of the inverter are controlled to extract the maximum power from solar panel during running at different levels of irradiance and temperatures using a Teaching Learning Based Optimization (TLBO) algorithm with minimum motor losses. The ratio of voltage magnitude and frequency is held within rated values to avoid saturation and motor overheating. The rating of PV array is chosen to develop the rated power of the pump at normal irradiance and temperature. The output voltage of the inverter is controlled during starting to prevent an excessive current from PV and to develop a torque larger than pump torque. An ANN is developed to give an optimal inverter voltage and frequency to extract maximum power from the PV array. The complete model is simulated using MATLAB/ Simulink.

Key-Words: - Photovoltaic panel, Water Pumping System, Three phase Induction Drive, TLBO, ANN

1 Introduction

Due to the increasing demands for energy around the world and the expecting end of fossil fuel; renewable energy sources gained a great attention as alternatives. Photovoltaic system (PV) has become one of the most important clean energy sources. A PV system is based on PV cell which produces a direct current when the solar radiation falls on its surface. One of the most important PV applications today is for pumping the water in remote areas [1] as it raises water from a well or spring and stores it in a tank for irrigation purpose. The PV-water pump system operation differs from that of the AC Mains powered pump, as they work under varying input power conditions. Many previous studies in the point of optimal operation of the PV-water pump system have been presented. An optimal strategy for operating the PV pumping system based on an induction motor driving a centrifugal pump has been introduced in [2, 3]; it has been achieved by maximizing the motor efficiency and minimizing the machine losses. A hybrid GA-ANN algorithm has been introduced in [4] for minimizing the converter losses inserted in a PV system coupled with an induction motor. The matching of an induction motor driven water-pumping system to PV array in order to transfer maximum energy has been given in [5]; a double step-up converter and six-step voltage source inverter have been embedded in this work. In [6] a fuzzy optimization approach to maximize the global efficiency of a PV water pumping system, maximize the speed of drive and increase the water discharge rate has been introduced; the study is based on three topologies for driving the water pump; driven by DC motor, permanent magnet synchronous motor or by an induction motor. The optimal performance of the PV-water pump system driven by DC motor at different patterns of solar radiation and ambient temperature has been analyzed in [7, 8]. An optimization approach based on the detection of the optimal power flow between the PV system and water pump through the usage of maximum power point tracker has been given in [9]. Takagi-Sugeno fuzzy approach has been developed in [10] to extract the maximum power from the PV system feeding a water pump via Dc motor. The usage of DC and induction motor as a part of multi and single stage water pump system has been reviewed in [11]; additionally the various techniques of MPPT have been introduced. A single stage water pumping system comprises PV array, six-step square wave

inverter, induction motor and centrifugal pump has been presented in [12]. The maximum power of the PV array has been obtained by operating the inverter as variable frequency; additionally the losses due to switching process have been minimized. An optimal design algorithm based on photovoltaic opportunity irrigation (POI) applied on several sub-models represented PV generator, variable speed centrifugal pump and olive orchard has been implemented in [13]. An optimized stand-alone solar pumping system has been implemented in [14]; the objective of this algorithm is to maximize the PV array efficiency using maximum power point tracking algorithm and minimize the induction motor losses. A linear actuated water pump driven by solar system has been optimized in [15] to suit the PV power characteristic and hydraulic requirements. An optimization process for maximizing the quantity of water pumped from the water pump system driven from an induction motor with improving the induction motor efficiency by obtaining an optimum voltage-frequency relation to control the motor has been introduced in [16]; additionally the impact of changing the PV array temperature has been studied. The performance of induction motor-pump system for irrigation purpose supplied from PV system has been studied in [17, 18].

In this paper a Teaching Learning Based Optimization (TLBO) technique is used to have the optimal values of inverter voltage and frequency to obtain a maximum power from PV and to minimize the losses of three phase induction motor drives a centrifugal water pump. ANN is built up to have PV maximum power point at any solar radiation and temperature. This maximum PV power is used as an input signal for other ANN to give optimal inverter voltage and frequency after trained by data obtained from TLBO algorithm. The field weakening method of reduced voltage and constant frequency is used to start the induction motor to avoid high starting current from PV. The complete system of PV array, three level inverter, three phase induction motor and centrifugal pump is simulated by MATLAB/ Simulink.

2 Mathematical Model

The system under study consists of photovoltaic array consists of a number of modules type First Solar FS-272, formed by the interconnection 8 series connected modules per string and 3- parallel strings, 3- level three phase inverter, 1.1kW three phase induction motor and water pump load. The mathematical model of each part is given in this section.

2.1 PV array model

The PV cell is simulated by a parallel current source represents the photon current connected in parallel with a diode and resistance, all in series with series resistance as shown in Fig. 1.

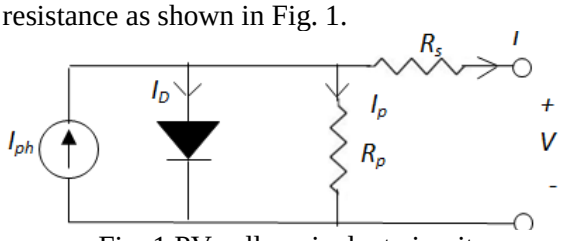

Fig. 1 PV cell equivalent circuit

The PV cell output current is given as follows [19, 20]:

$$I = I_{ph} - I_D - I_p \quad (1)$$

$$I = I_{ph} - I_o \left\{ exp\left(\frac{V+IR_s}{\alpha V}\right) - 1 \right\} - \left\{\frac{V+IR_s}{R_p}\right\} \quad (2)$$

Where: I_{ph} is the photon current which is generated by the sunlight strikes the PV cell surface, I_o is the saturation current of the diode, V and I are the cell voltage and current respectively, R_s and R_p are the cell series and parallel resistances respectively, α is the ideality factors of the diode and V_T is the thermal voltages of the diode. The PV array is formulated by connecting N_{ss} PV modules in series and N_{pp} parallel strings as shown in Fig. 2, the current supplied from the PV array is written by:

$$I_{arr} = N_{pp} I_{ph} - N_{pp} I_o \left\{ exp\left(\frac{V+IR_{sarr}}{\alpha N_{ss} V_T}\right) - 1 \right\} - \left\{\frac{V+IR_{sarr}}{R_{parr}}\right\} \quad (3)$$

Where R_{sarr} and R_{parr} are the series and parallel resistances of the PV array and given by [21]:

$$\begin{cases} R_{sarr} = \left(\frac{N_{ss}}{N_{pp}}\right) N_s R_s \\ R_{parr} = \left(\frac{N_{ss}}{N_{pp}}\right) N_s R_p \end{cases} \quad (4)$$

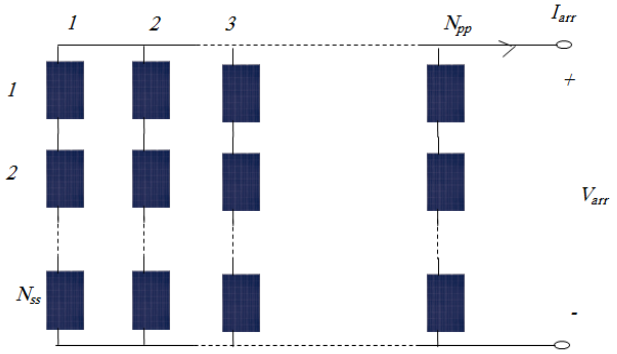

Fig. 2 The arrangement of a PV array [21]

2.2 three level three phase inverter model

The three-level inverter consists of three arms of power switching devices. Each arm consists of four switching devices along with their antiparallel diodes and two neutral clamping diodes as shown in

the Fig. 3 [22]. The switching states of one phase three level inverter are listed in Table 1.

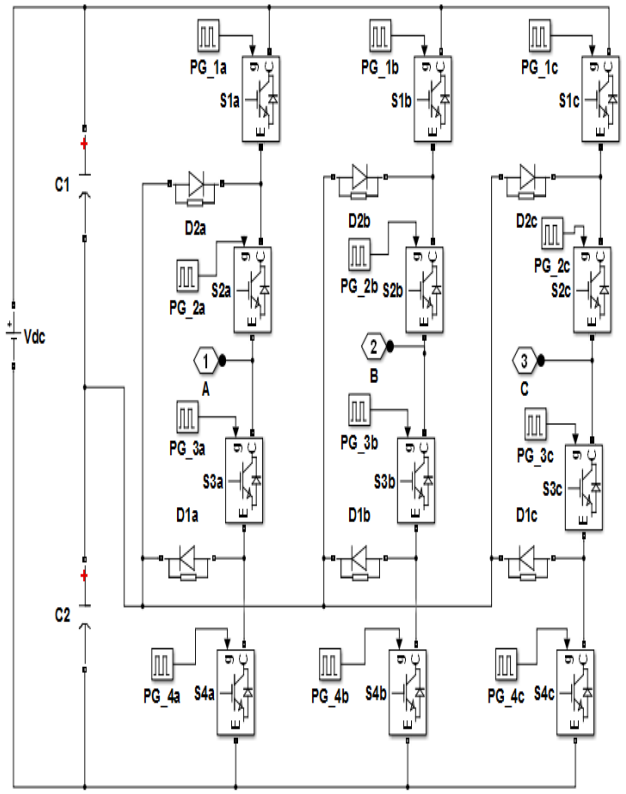

Fig. 3 Three Level inverter construction

Table 1 Switching states for one phase of three level inverter

Output Voltage	S_1	S_2	S_3	S_4
$0.5V_{dc}$	1	1	0	0
0	0	1	1	0
$-0.5V_{dc}$	0	0	1	1

The rms value of the fundamental line voltage of the inverter is given as:

$$V_{L\,L\,rms} = m\,\frac{\sqrt{3}}{\sqrt{2}}0.5V_{dc} = 0.6124\,m\,V_{dc} \quad (5)$$

Where: m is the modulation index which controls the amplitude of the fundamental component of the output voltage of the inverter. The modulation index must be greater than 0 and lower than or equal to 1.

There are advantages in the application of the three level neutral point clamped inverters fed three phase induction motor over conventional two level inverters as the three level inverter can reduce harmonics in the output voltage and current due to the multilevel output voltage. [23].

2.3 three phase induction motor model

The mathematical model of squirrel cage three phase induction motor in the d-q frame is given as: [24]

The stator voltage equations are:

$$V_{dS} = i_{dS}R_s + \frac{d}{dt}\lambda_{dS} - \omega_S\lambda_{qS} \quad (6)$$

$$V_{qS} = i_{qS}R_s + \frac{d}{dt}\lambda_{qS} + \omega_S\lambda_{dS} \quad (7)$$

Where: V_{dS} is d-axis stator voltage, V_{qS} is q-axis stator voltage, i_{dS} is d-axis stator current, i_{qS} is q-axis stator current, R_s is stator winding resistance, λ_{dS} is d-axis stator flux linkage, λ_{qS} is q-axis stator flux linkage and ω_S synchronous speed in rad/s.

The rotor voltage equations are:

$$0 = i_{dR}R_R + \frac{d}{dt}\lambda_{dR} - (\omega_S - \omega)\lambda_{qR} \quad (8)$$

$$0 = i_{qR}R_R + \frac{d}{dt}\lambda_{qR} + (\omega_S - \omega)\lambda_{qR}\lambda_{dR} \quad (9)$$

Where: i_{dR} is d-axis referred rotor current, i_{qR} is q-axis referred rotor current, R_R is referred rotor winding resistance, λ_{dR} is d-axis rotor flux linkage, R_R is q-axis rotor flux linkage and ω is the rotor speed in rad/s.

The flux linkages are defined by:

$$\lambda_{dS} = L_S i_{dS} + M i_{dR} \quad (10)$$

$$\lambda_{qS} = L_S i_{qS} + M i_{qR} \quad (11)$$

$$\lambda_{dR} = L_R i_{dR} + M i_{dS} \quad (12)$$

$$\lambda_{qR} = L_R i_{qR} + M i_{qS} \quad (13)$$

Where: L_S is self- inductance of stator winding, L_R is referred self-inductance of rotor winding, M is mutual inductance

The electromagnetic torque equation is:

$$T_e = \frac{3}{2}\frac{p}{2}M\left(i_{qS}i_{dR} - i_{dS}i_{qR}\right) \quad (14)$$

The mechanical equation of the motor and the load is:

$$T_e - T_L = J\frac{d\omega}{dt} + B\omega \quad (15)$$

Where: J is moment of inertial in kg.m^2, and B friction N.m.s.

The practical characteristic of 1.1 kW, 1440 rpm (150.8 rad/s) centrifugal pump can be given as:[25]

$$T_L = 0.7634 - 0.0461\,\omega + 0.0011\,\omega^2 + 0.000003273\,\omega^3 \quad (16)$$

Where ω is pump speed in rad/s.

3 Characteristics of the proposed System

The proposed water pump system consists of a photovoltaic array which acts as a power supply source, connected to a pulse width modulation (PWM) 3-level three phase inverter, which converts the DC voltage to variable voltage variable frequency AC voltage in order to feed a three-phase induction motor. The complete system description is shown in Fig. 4.

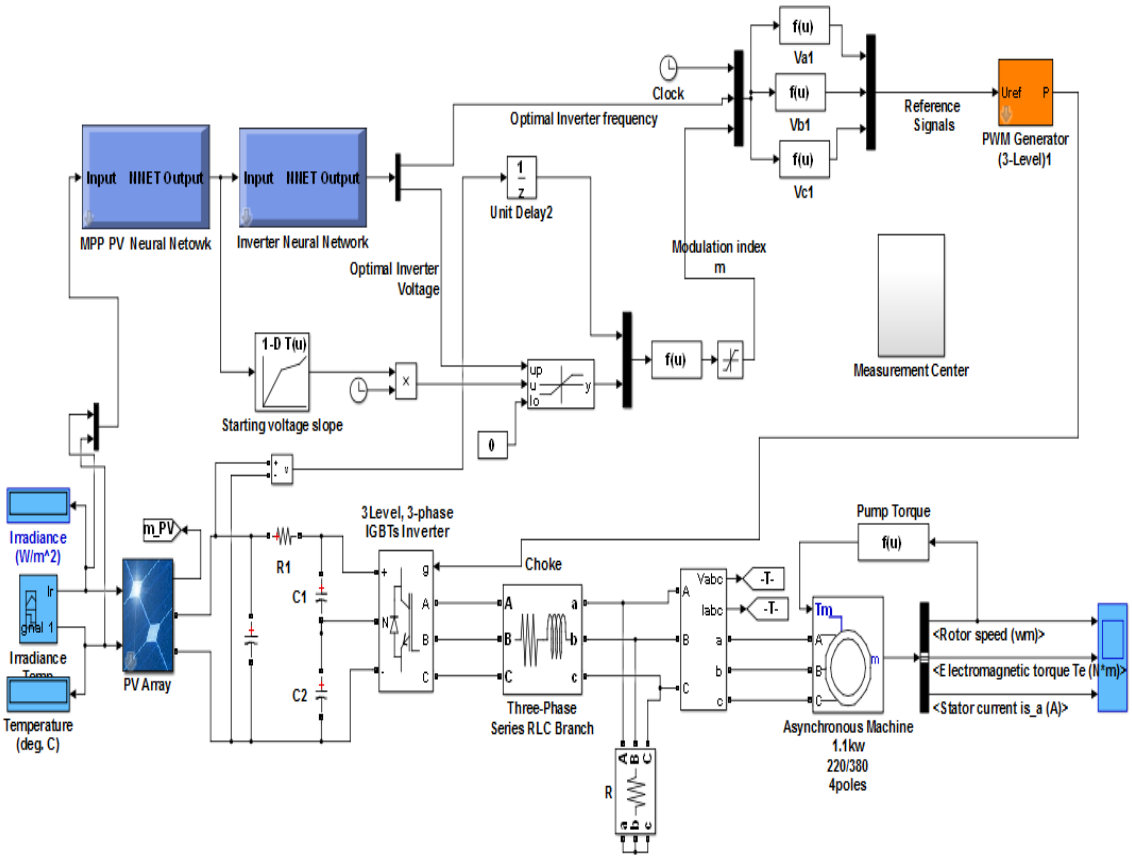

Fig. 4 System Description

3.1 PV array model Characteristics

A photovoltaic array consists of a number of modules type First Solar FS-272, formed by the interconnection 8 series connected modules per string and 3 parallel strings, connected to provide the required voltage and current. The characteristics of one module at 25 °C are shown in Fig. 5. The module specification are: number of cells per module are 116, open circuit voltage is 94.5738 V, short circuit current is 1.181 A, voltage at maximum power point is 70.558 V, current at maximum power point is 1.0109 A. The characteristics of the total array are shown in Fig. 6. A neural network is designed to give the maximum PV power at certain solar radiation and ambient temperature. The ANN has two input layers of solar radiation and temperature and one output layer of maximum PV power. Practical data of solar radiation and ambient temperature measured by solar radiation and meteorological station located at National Research Institute of Astronomy and Geophysics Helwan, Cairo, Egypt are used to extract the PV MPP which is a target of ANN model. The variation of mean square error of the network with epochs is shown in Fig. 7.

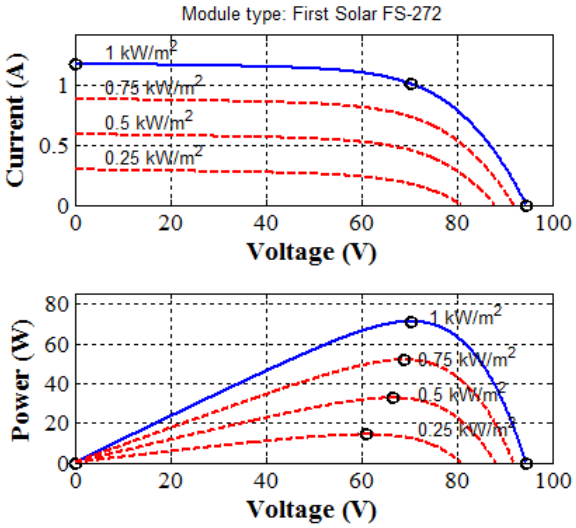

Fig. 5 I-V and P-V characteristics of one PV module

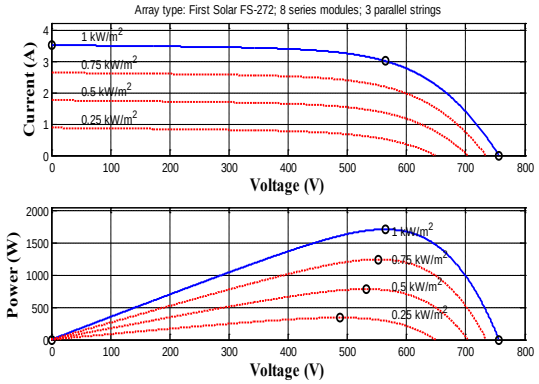

Fig. 6 I-V and P-V characteristics of total array

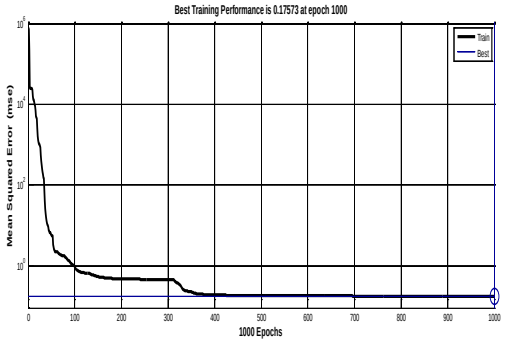

Fig. 7 Variation of PV MPP ANN mean square error with epochs

3.2 water pump induction motor characteristics

In water pump induction motor system; the output power of the pump can be controlled by the variation of the motor voltage and frequency. The parameters of 4- pole, 220/380 V, 1.1 kW, 50Hz three phase induction motor used to drive the water pump are listed as follows:

Stator resistance = 7.4826 Ω, stator leakage inductance= 0.0221 H,

Referred rotor resistance = 3.6840 Ω, referred rotor leakage inductance = 0.0221 H,

Magnetizing inductance = 0.4114 H, Core loss resistance=2400 Ω, Moment of Inertia= 0.02 kg.m^2,

The performance characteristics of the motor with V/f control method are given to determine the required motor input power to drive the water pump at different speed. Fig. 8 shows the variation of motor developed torque and water pump torque with speed at V/f control. The operating speeds are the intersections of both motor and pump torques. Fig. 9 shows the variation of motor current with speed at different frequencies. It's shown that the starting current is higher than normal operating current and this starting current is higher than the short circuit current of the PV panel. Therefore stator voltage should be controlled during starting to limit the starting current provided that the motor torque is higher than the pump power and starting current is lower than short circuit current of PV array. The optimal slope of increasing voltage at different levels of solar radiation and temperature are obtained using TLBO algorithm as shown in Table 1. The variation of motor input power with speed is shown in Fig. 10. The input power at lower frequencies is lower than one of rated frequency. Therefore, at different PV maximum power with different temperatures and irradiances, the inverter voltage and frequency are controlled to match drive power with PV maximum power.

Table 1 Optimum starting slope on inverter voltage

Maximum PV Power	Slope
340.6	8
784.1	25
1245	28
1400	31

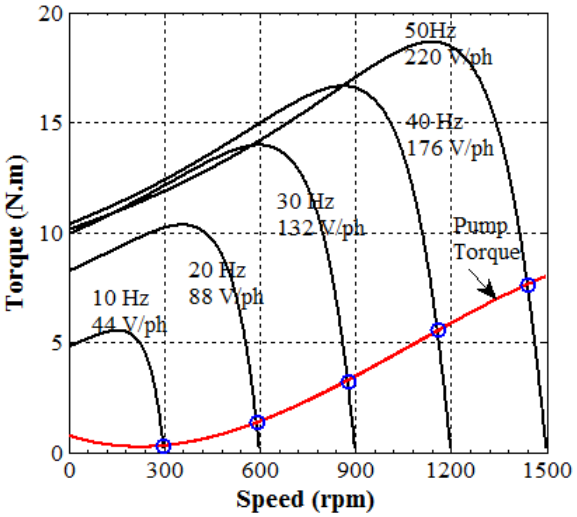

Fig. 8 Variation of motor developed torque and pump torque with speed

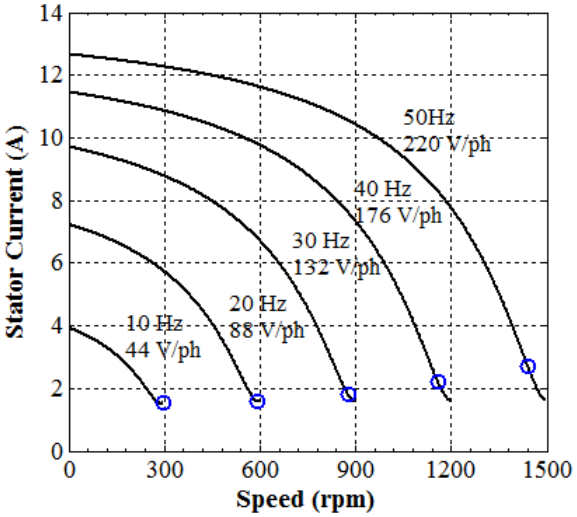

Fig. 9 Variation of motor current torque with speed

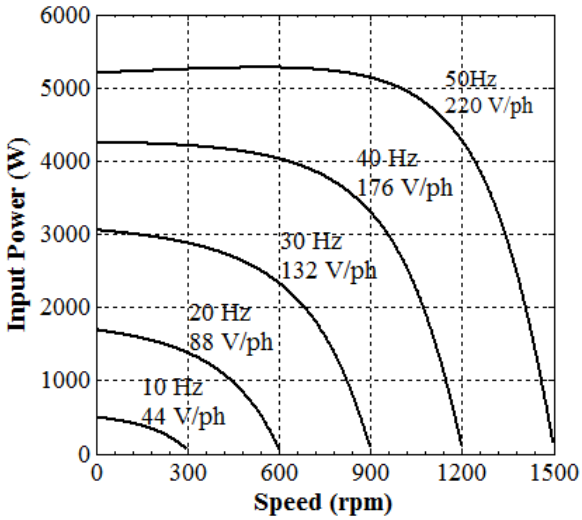

Fig. 10 Variation of motor input power with speed

4 Teaching learning based optimization algorithm (TLBO)

TLBO is a new meta-heuristic optimization algorithm that has been developed by R.V. Rao et al. [26]. It has been advisable to use TLBO in finding the global optimal solutions for continuous and nonlinear functions as it requires less computational time and gives high accurate results. The teaching process used in TLBO algorithm is based on the interaction between the teacher in a teaching class with students which is known as teacher phase and the interaction between two groups of students which is known as learner phase; through these two phases of learning the global optimal solution is obtained. A good teacher results in good learners as teacher is considered as the best person that transfers his knowledge to the learners. The main advantages of TLBO algorithms have been mentioned in [27]; it needs less controlling parameters such as the size of population, number of generations and number of iterations, additionally it is reliable algorithm that guarantees the obtaining of optimal solution not local one and easier than other meta-heuristic algorithms.

4.1 teacher phase

In this stage of learning process; the students are learned through the teacher which is considered as the person has the most experience and knowledge in a subject, therefore the teacher is considered as the best (optimal) solution in the class room population. Practically the teacher moves the mean of his/her knowledge to the class based on the capability of the class and cannot move his/her full knowledge. One can describe the difference between the teacher result and mean result of learners as follows [26]:

$$Diff\_Mean_i = r_i(M_{new} - T_F M_i) \quad (17)$$

Where M_{new} is the new obtained mean of the teacher after moving its mean knowledge to learners, M_i is the mean of transferred knowledge from teacher to students, r_i is a random value in range [0, 1] and T_F is the teaching factor which control the mean value to be changed. The value of T_F can be either 1 or 2 based on the following equation:

$$T_F = round\,[1 + rand(0,1)\{2-1\}] \quad (18)$$

Based on the difference between two means given in eqn. 17; the value of solution is updated as follows:

$$x^{new}{}_i = x^{old}{}_i + Diff\_Mean_i \quad (19)$$

Where $x^{new}{}_i$ is the updated solution, $x^{old}{}_i$ is the old solution. The new solution is accepted if its fitness function is better than the previous one. The accepted solution acts as input to the second stage of learning process which is learner phase.

4.2 learner phase

In this stage of learning process; the knowledge is transferred to a group of students through the interaction with another group. In order to explain the learner phase, it is assumed that there are two groups of student group i and group j, with knowledge x_i and x_j, at the beginning of this process the fitness function of both groups are calculated and compared such that the knowledge has been updated based on the following formula:

$$x^{new}{}_i = x^{old}{}_i + r_i(x_i - x_j) \quad if\ fit(x_i) < fit(x_j) \quad (20)$$

$$x^{new}{}_i = x^{old}{}_i + r_i(x_j - x_i) \quad if\ fit(x_j) < fit(x_i) \quad (21)$$

Where *fit* (x_i) and *fit* (x_j) are the fitness function of group i and j respectively. The updated solution, $x^{new}{}_i$, is accepted if its fitness function is better than the previous one. The flow chart represents the main steps of TLBO algorithm is given in Fig. 11.

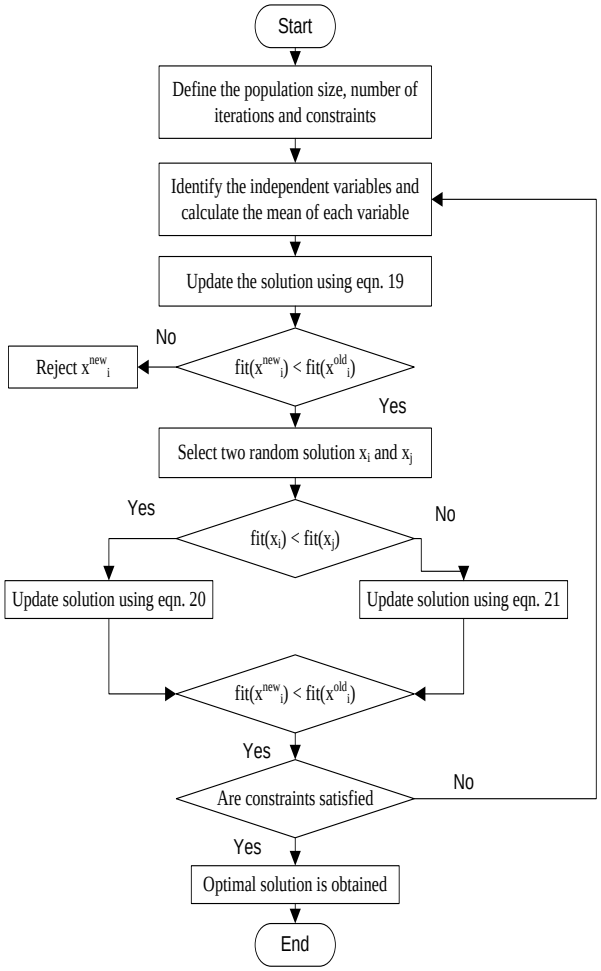

Fig. 11 The main steps of TLBO algorithm

5 Numerical Analysis

The Teaching Learning Based Optimization method is used to obtain the optimal inverter voltage and frequency for certain maximum PV power to drive the water pump with minimum motor losses. The Objective function is to minimize the motor losses with following constraints:

- Abs (input power – PV maximum power) < 1
- Abs (developed torque – Pump torque) <=0.01
- V/f < =(V_{rated}/f_{rated})

The TLBO parameters used are population size =50, maximum number of generations=200, Variable numbers=3. The design variables are frequency, voltage and slip. For each maximum power of solar panel the TLBO program is run for 20 times and the best result is recorded as shown in Fig. 12 and Fig. 13

The variation of TLBO objective function for maximum power of 1300 W is shown in Fig. 14 for 20 running times. The ranges of TLBO variables frequency, voltages and slip respectively are lower limit = [45 180 .0001] and upper limit = [50 220 0.4].

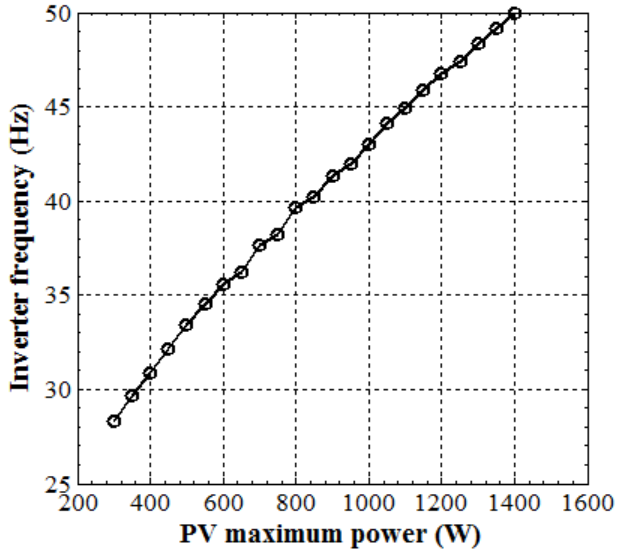

Fig. 12 Variation of optimal inverter frequency with PV maximum power

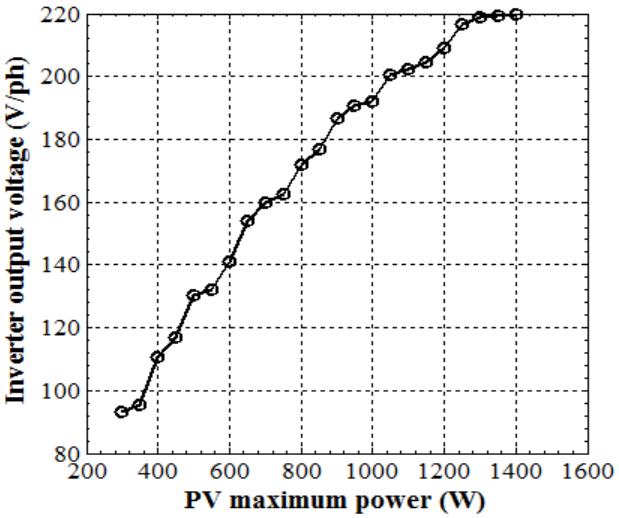

Fig. 13 Variation of optimal inverter output voltage with PV maximum power

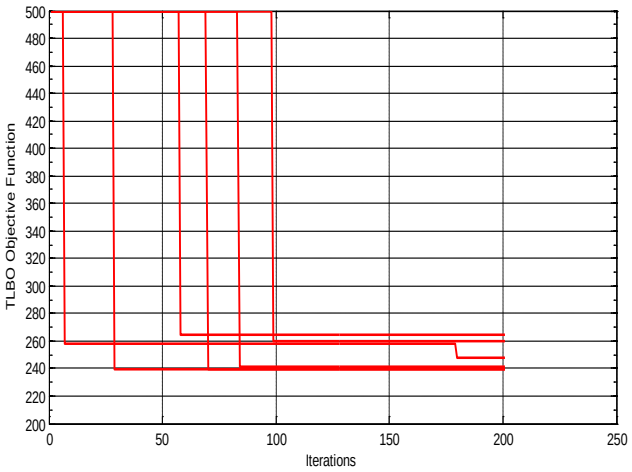

Fig.14 Variation of the TLBO objective function with iterations

A feed-forward back propagation ANN is designed to give the optimal inverter voltage and frequency. The input of ANN is PV maximum power and the outputs of ANN are inverter voltage and frequency. The data of optimal voltage and frequency at each PV maximum power which are obtained using TLBO method are used as training data of ANN. The variation of mean square error is shown in Fig. 15.

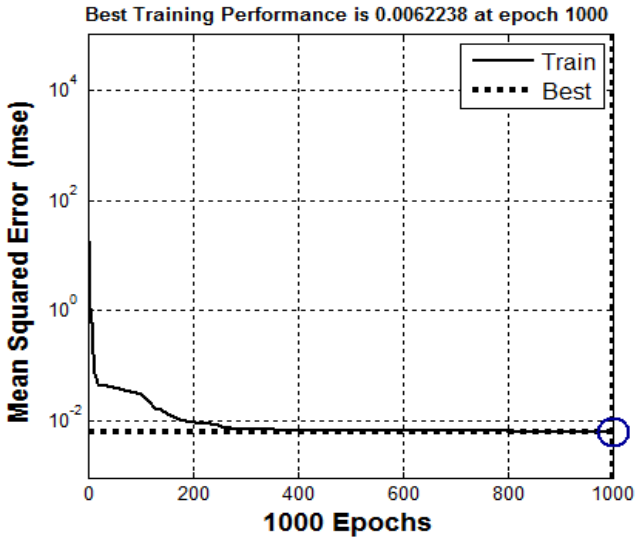

Fig. 15 Variation of ANN mean square error with epochs

After training of the ANN, the maximum PV power is the input to the trained ANN and the outputs are the inverter voltage and frequency.. The variation of simulated result, target and the error between them are shown in Fig 16 and Fig.17.

The variation of motor efficiency with input power is shown in Fig. 18. The efficiency of the proposed method which adjusts the inverter voltage and frequency to obtain the maximum power from PV and runs the induction motor with minimum losses is higher than that of V/f method especially at light input powers. The motor efficiencies of two methods are very close for input power greater than 600 W.

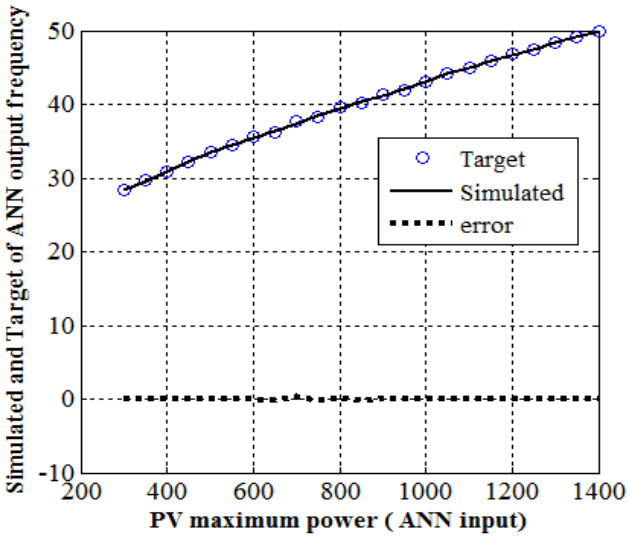

Fig. 16 Variation of ANN output frequency

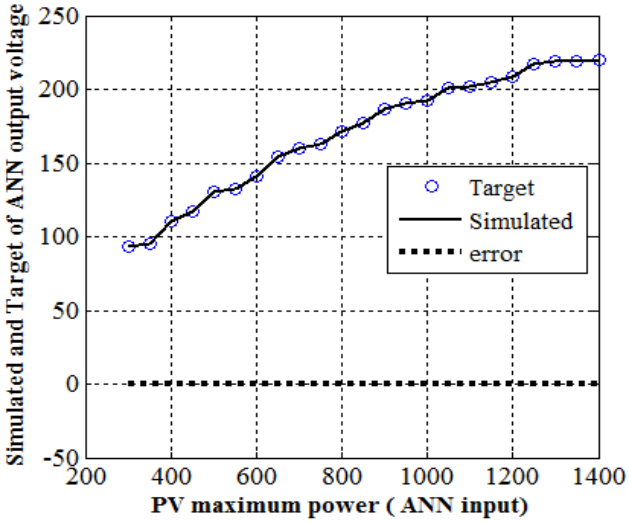

Fig. 17 Variation of ANN output voltage

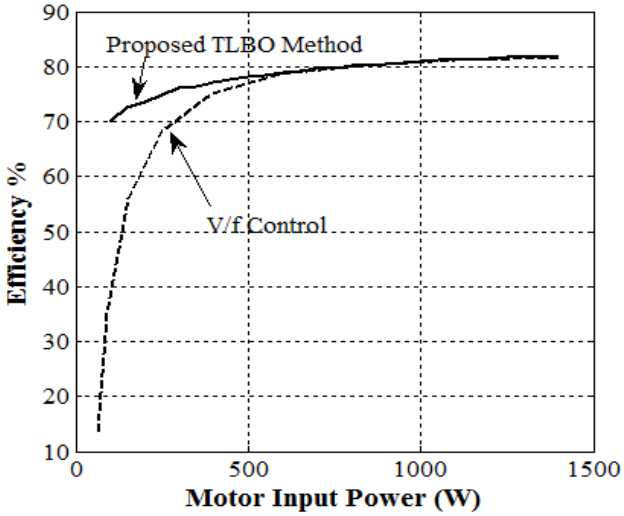

Fig. 18 Variation motor efficiency with input power with proposed and V/f methods

The performance characteristics of the system under solar radiation changes as 500 W/m^2 from start up to 20 s, 750 W/m^2 from 20 s to 30 s and 500 W/m^2 from 30 s to 40 s. as shown in Fig. 19 with constant temperature at 25 °C. The variation of inverter frequency and voltage are shown in Figs. 20 and 21. During starting the frequency is fixed at 39 Hz which is obtained from Inverter ANN and the inverter voltage is increased with slope 25 which are obtained using TLBO algorithm when maximum PV is 784 W at G=500 W/m2 and T=25 °C. The output current, voltage and power of the PV array are shown in Figs. 22, 23 and 24 respectively. Fig. 25 shows the variation of motor speed with time. It's shown that the motor speed is increased with solar radiation due to increasing of the inverter frequency. The variation of motor and load pump torque with time is shown in Fig. 26.

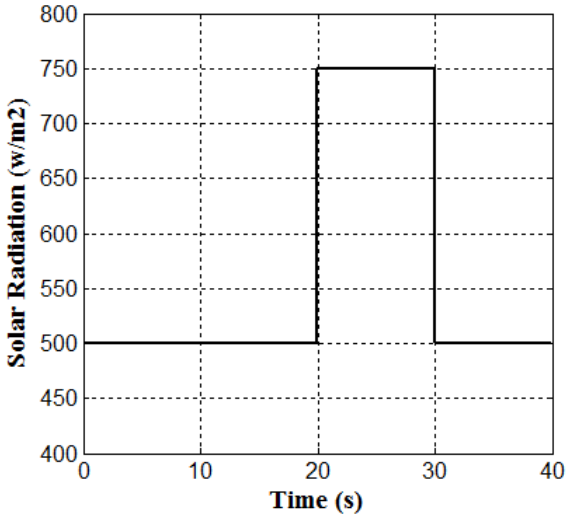

Fig. 19 Variation of solar radiation with time

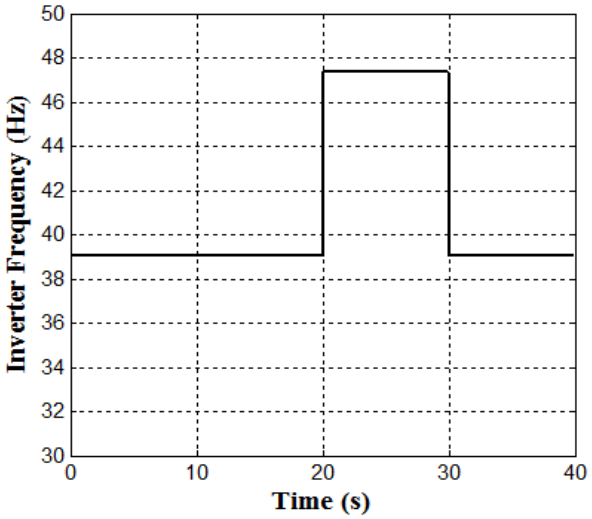

Fig. 20 Variation of Inverter frequency with time

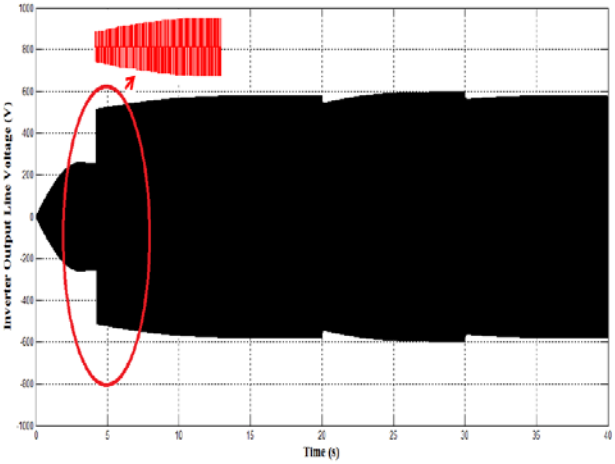

Fig. 21 Variation of Inverter output voltage with time

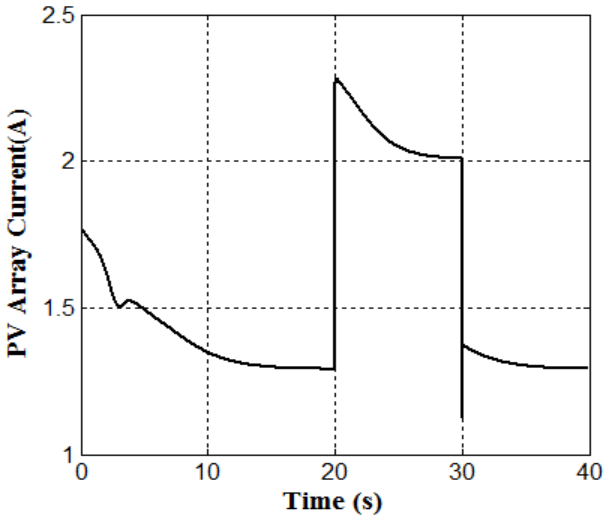

Fig. 22 Variation of PV array current output voltage with time

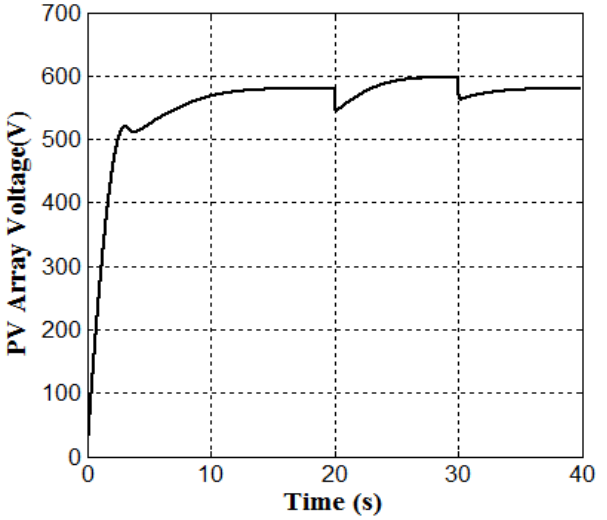

Fig. 23 Variation of PV array voltage output voltage with time

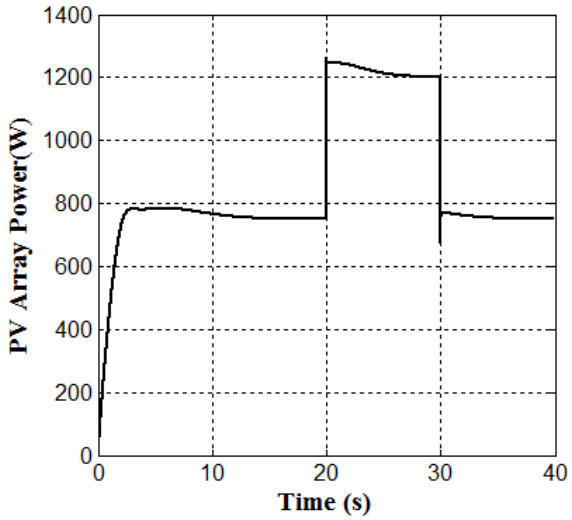

Fig. 24 Variation of PV array power with time

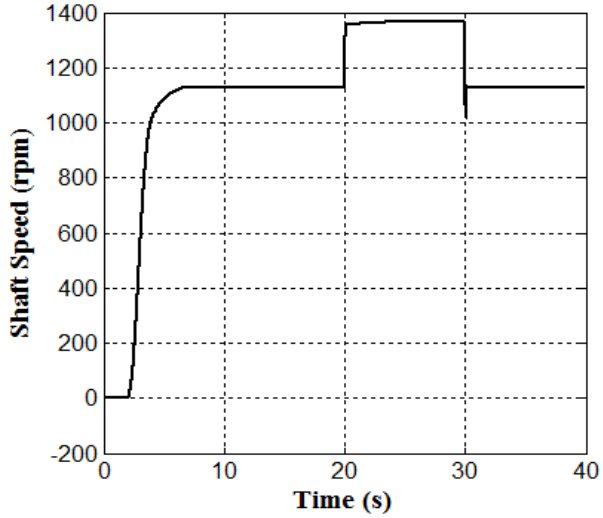

Fig. 25 Variation of pump speed with time

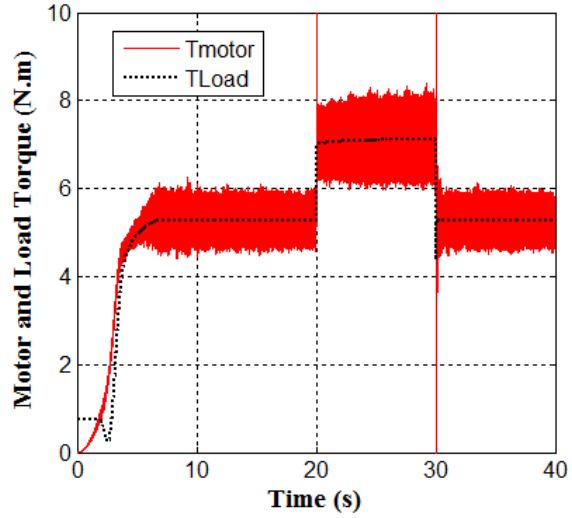

Fig. 26 Variation of motor and pump torque with time

6 Conclusion

In this paper an optimal performance of water pump induction motor connected directly to PV array using three level inverter without storage system is presented. The optimal performance is achieved by controlling the inverter voltage and frequency to obtain maximum power from PV with minimum motor losses using Teaching Learning Based Optimization(TLBO) technique. ANN is built up to have PV maximum power point at any solar radiation and temperature. This maximum PV power is used as an input signal for other ANN to give optimal inverter voltage and frequency after training by data obtained with TLBO method. The optimal slope of increasing inverter output voltage with constant frequency during starting is obtained using TLBO algorithm. The whole system of PV array, three level inverter, three phase induction motor and centrifugal pump is modeled using MATLAB/ Simulink and tested under different radiations. After simulation the optimal inverter voltage and frequency to obtain PV maximum power with minimum motor losses are obtained and ANN is built up to make the controller adaptive at different solar radiation and temperatures.

References:

[1] Masters G. M. Renewable and efficient electric power systems. John Wiley & Sons, Inc., Hoboken, New Jersey, 2004.

[2] Betka A., Attali A. Optimization of a photovoltaic pumping system based on the optimal control theory. Solar Energy 2010; 84, pp.1273–1283.

[3] Betka A., Moussi A. Performance optimization of a photovoltaic induction motor pumping system. Renewable Energy 2004; 29, pp. 2167–2181.

[4] Kulaksız A., Akkaya R. A genetic algorithm optimized ANN-based MPPT algorithm for a stand-alone PV system with induction motor drive. Solar Energy 2012; 86, pp. 2366–2375.

[5] Akbaba M. Matching induction motors to PVG for maximum power transfer. Desalination 2007; 209, pp. 31–38.

[6] Benlarbi K., Mokrani L., Nait-Said M. A fuzzy global efficiency optimization of a photovoltaic water pumping system. Solar Energy 2004; 77, pp. 203–216.

[7] Ghoneim A. Design optimization of photovoltaic powered water pumping systems. Energy Conversion and Management 2006; 47, pp. 1449–1463.

[8] Jaziri S., Jemli K. Optimization of a photovoltaic powered water pumping system. International

Conference on Control, Decision and Information Technologies, 6-8 May 2013, pp. 422–428

[9] Badoud A., Khemliche M., Bouamama B., Bacha S., Villa L. Bond graph modeling and optimization of photovoltaic pumping system: Simulation and experimental results. Simulation Modelling Practice and Theory2013; 36, pp. 84–103.

[10] Ouachani I., Rabhi A., Tidhaf B., Zouggar S., Elhajjaji A. Optimization and control for a photovoltaic pumping system. International Conference on Renewable Energy Research and Applications, Madrid, Spain, 20-23 October 2013, pp. 734–739.

[11] Periasamy P., Jain N., Singh I. A review on development of photovoltaic water pumping system. Renewable and Sustainable Energy Reviews 2015; 43, pp. 918–925.

[12] Muljadi E. PV water pumping with a peak-power tracker using a simple six-step square-save inverter. IEEE Transactions on industrial applications 1997; 33(3), pp. 714–721.

[13] Luque R., Reca J., Martinez J. Optimal design of a standalone direct pumping photovoltaic system for deficit irrigation of olive orchards. Applied Energy 2015; 149, pp. 13–23.

[14] Corrêa T., Jr. S., Silva S. Efficiency optimization in stand-alone photovoltaic pumping system. Renewable Energy 2012; 41, pp. 220–226.

[15] Wade N., Short T. Optimization of a linear actuator for use in a solar powered water pump. Solar Energy 2012; 86, pp. 867–876.

[16] Betka A., Moussi A. Optimized solar water pumping system based on an induction motor driving a centrifugal pump. European Power and Energy Systems, June 15 – 17, 2005, Benalmádena, Spain.

[17] Gumus B., Yakut Y. Analysis of induction motor-pump system supplied by a photovoltaic generator for agricultural irrigation in southeastern Anatolian region of Turkey. Journal of Electrical Engineering & Technology 2015; 10, pp. 742-750.

[18] Belgacem B. Performance of submersible PV water pumping systems in Tunisia. Energy for Sustainable Development 2012; 16, pp. 415–420.

[19] El-arini M., Othman A., Fathy A. A new optimization approach for maximizing the photovoltaic panel power based on genetic algorithm and lagrange multiplier algorithm. International Journal of Photoenergy 2013, pp. 1–12.

[20] Fathy A., El-arini M., Othman A. A New evolutionary algorithm for the optimal sizing of stand-alone photovoltaic system based on genetic algorithm. International Review of Electrical Engineering 2013; 8(3), pp. 1067–1075.

[21] Fathy A. Reliable and efficient approach for mitigating the shading effect on photovoltaic module based on modified artificial bee colony algorithm. Renewable Energy 2015; 81, pp. 78–88.

[22] Rajesh B., Manjesh Dr. Analysis of THD and Harmonics in 3 Level Inverter with LC filter. ITSI Transactions on Electrical and Electronics Engineering 2014; 2(4), pp. 30– 34.

[23] Adrian S., Kokkosis A. Vector Control of Induction Machine Fed by Three Level Inverter. Journal of Eleetrieal and Eleetronies Engineering 2011; 4(1), pp. 215–218.

[24] Chiasson J. Modelling and high performance control of electric machines. John Wiley & Sons, Inc., 2005.

[25] ETAP11, Motor Load Model Library Model.

[26]Rao R., Savsani V., Vakharia D. Teaching–learning-based optimization: A novel method for constrained mechanical design optimization problems. Computer-Aided Design 2011; 43, pp. 303–315.

[27] Pawar P., Rao R. Parameter optimization of machining processes using teaching–learning-based optimization algorithm. International Journal of Advanced Manufacturing Technology 2013; 67(5), pp. 995– 1006.